Supplemental Materials

Molecular Biology of the Cell

Mazel et al.

Supplementary Material:

Supplementary Figures:

A

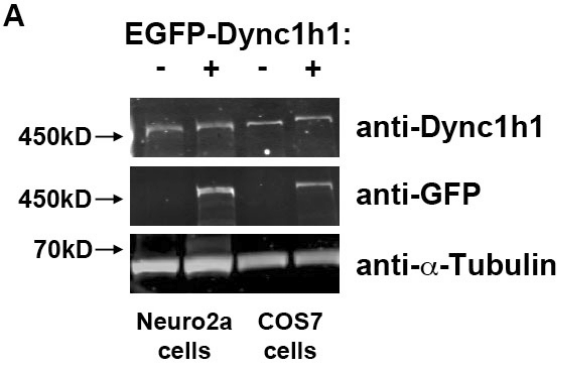

B

	Neuro2a cells	COS7 cells
transfection efficiency	32%	24%
ratio of EGFP-Dync1h1 in lysate to the endogenous Dync1h1	0.26	0.61
ratio of EGFP-Dync1h1 in individual cells to the endogenous Dync1h1	0.64	2.51

Figure S1: Estimation of EGFP-Dync1h1 expression levels. A) Western blot analysis of Neuro2a and COS7 cells. Cell lysates from untransfected or EGFP-Dync1h1 transfected cells were prepared and probed with antibodies recognizing total Dync1h1 (endogenous and EGFP fusion proteins), EGFP and α-tubulin as loading control. Transfection of EGFP-Dync1h1 under the control of the weak delCMV promoter lead to a very small increase in the total levels of Dync1h1. B) The ratio of EGFP-Dync1h1 to the endogenous Dync1h1 in individual cells was estimated by normalizing the ratio observed in lysates to transfection efficiencies.

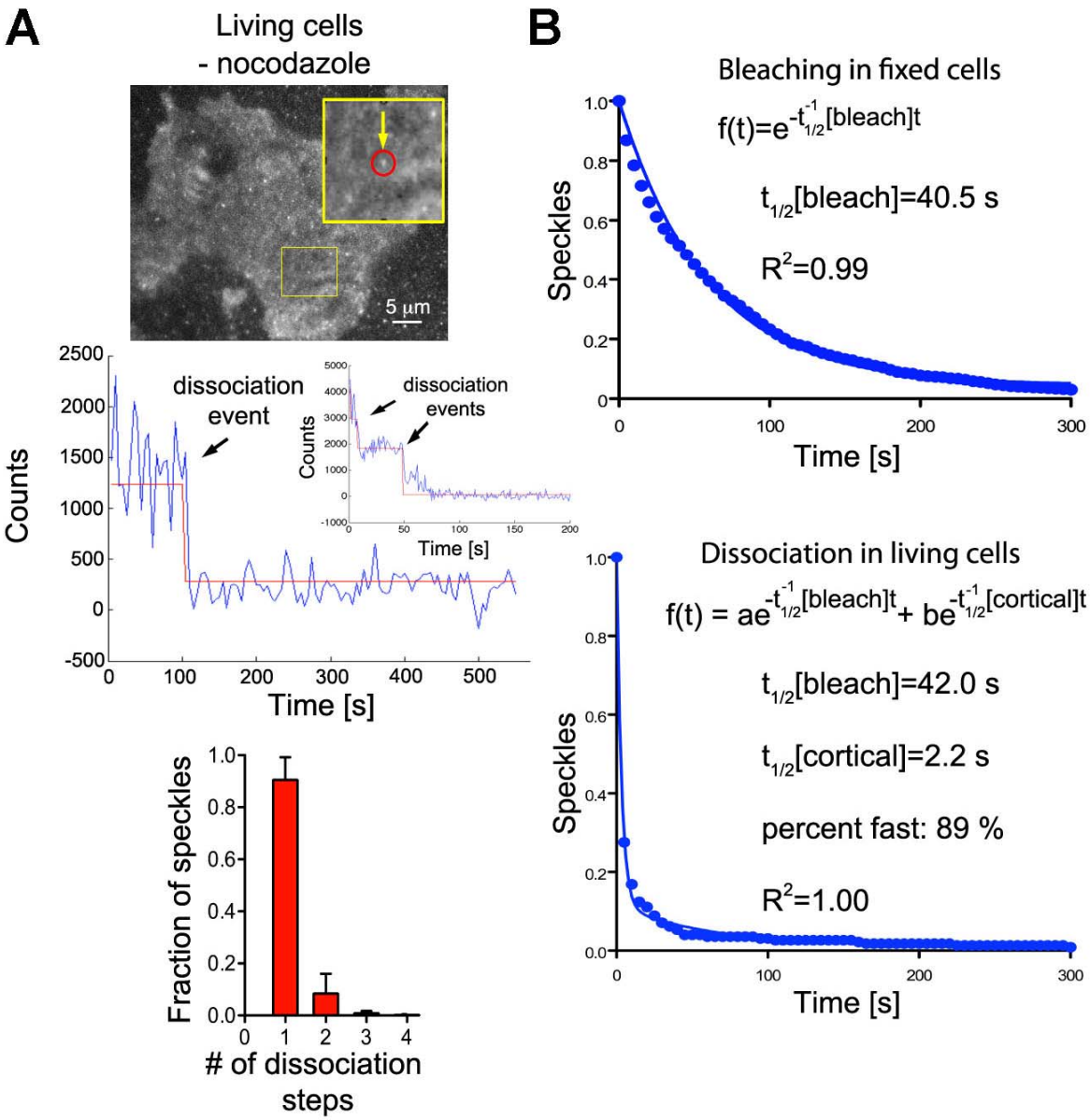

Figure S2: Turnover of dynein complexes at the cell cortex in living, unperturbed cells. A) Rapid dissociation of EGFP-labeled dynein heavy chain (Dync1h1) speckles from the cell cortex in living COS7 cells (top). The distribution of dissociation steps shows that speckles usually dissociate in a single step (bottom left; n=666 from 4 cells). B) Number of remaining, EGFP-Dync1h1 molecules plotted against time. In fixed cells, the bleaching kinetics of initially detected individual EGFP molecules fits well to a single exponential decay function. In living cells, the kinetics of EGFP-Dync1h1 dissociation does not fit a single exponential decay completely (R^2=0.97±0.004). Assuming similar bleaching kinetics in fixed and living cells, a fast component, which is due to dynamic interaction of dynein speckles with the cortex is detected using a double-exponential fit ($t_{1/2}$[cortical]=1.9±0.6 s, fraction fast: 0.77±0.13 n=666 speckles in 4 cells). The overall density of speckles was 0.20±0.04 (live cells) or 0.32±0.04 (fixed cells) speckles/µm^2; n=4 cells or n=3 cells).

In all analyses the same slow component $t_{1/2}$[bleach], which was based on the average value measured in fixed cells was used ($t_{1/2}$[bleach]=42±2 s, n=1982 speckles in 3 cells).

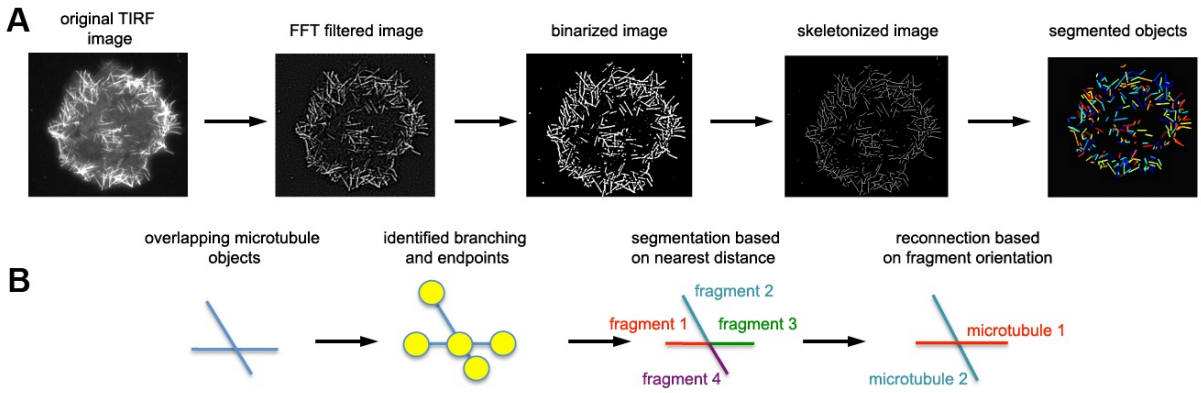

Figure S3: Procedure used for microtubule tracking. A) Original TIRF images were processed using a fast Fourier transform based band-pass filter, binarized, skeletonized and segmented to identify individual microtubule objects. B) Segmentation of overlapping microtubule objects was performed by first identifying branch-points and endpoints. Based on the distance between these points, the microtubule structures were segmented into smaller fragments. Microtubule objects were obtained by reconnecting these fragments based on their relative orientation.

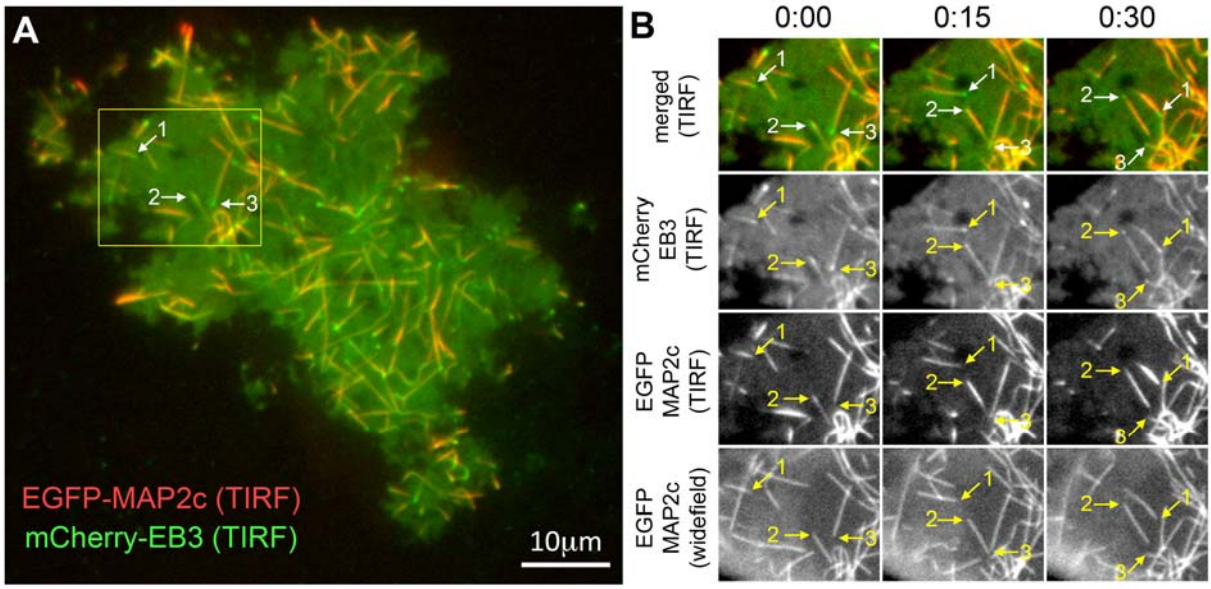

Figure S4: Polarity orientation of motile short microtubules. A) Representative image of a COS7 cell expressing EGFP-MAP2c and mCherry-EB3 obtained via TIRF microscopy. Numbered arrows point at 3 examples for short microtubules, which are labeled with the plus-tip marker EB3 at their leading ends. B) Image sequence showing directional movements of the 3 short microtubules indicated in A) (see also Movie 2). Due to the reduced MT polymerization in the presence of MAP2c, plus-end accumulation of EB3 was much less pronounced compared to cells that do not express MAP2c.

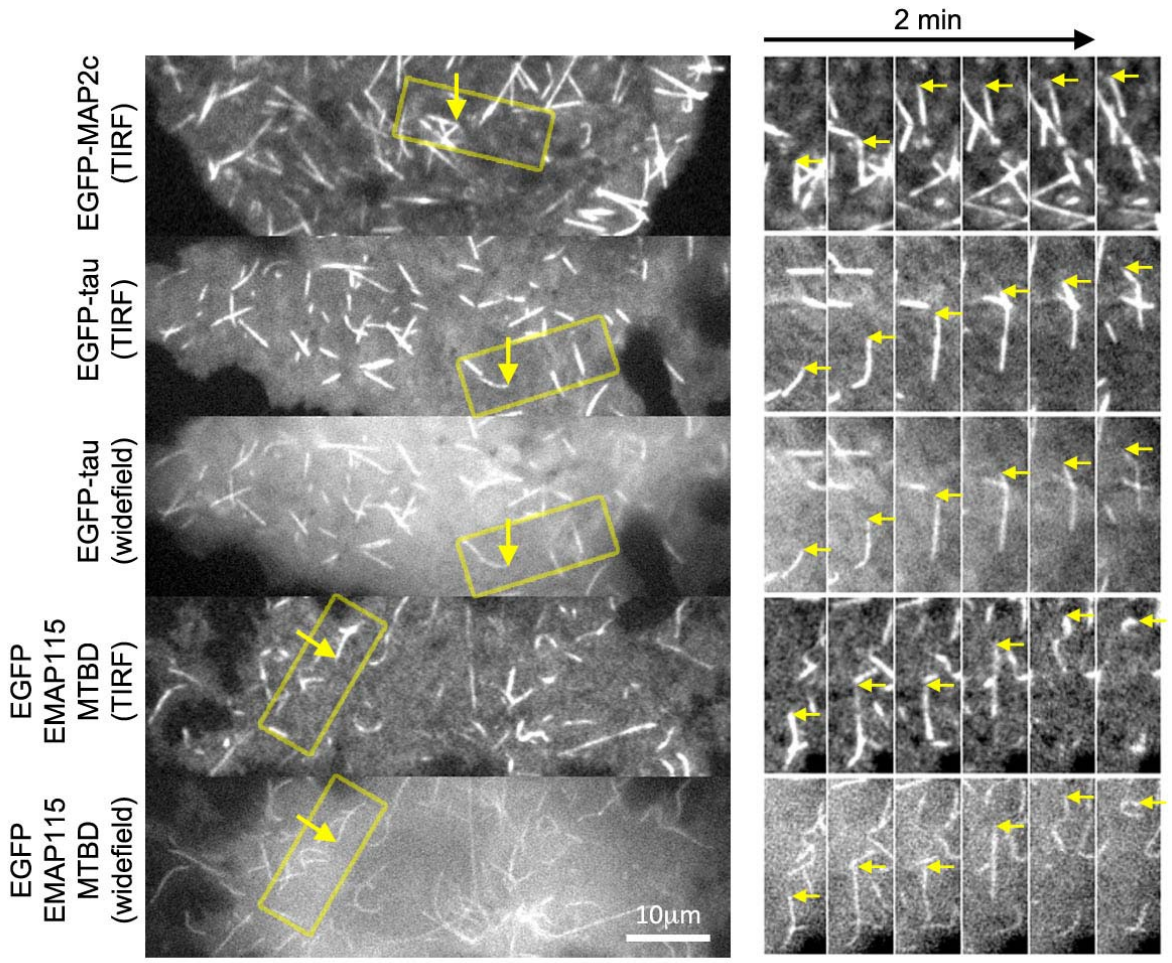

Figure S5: Directional sliding of microtubules in COS7 cells transfected with various microtubule associated proteins. COS7 cells were transfected with EGFP-MAP2c, EGFP-tau, or EGFP-EMAP115-MTBD (microtubule binding domain). Microtubule motility was observed either via wide-field or TIRF imaging shortly after nocodazole washout. Right: Overview images of representative cells. Left: Image sequences corresponding to the yellow boxes indicated on the right panels. Yellow arrows indicate the leading end of motile short microtubules (see also Movie 3).

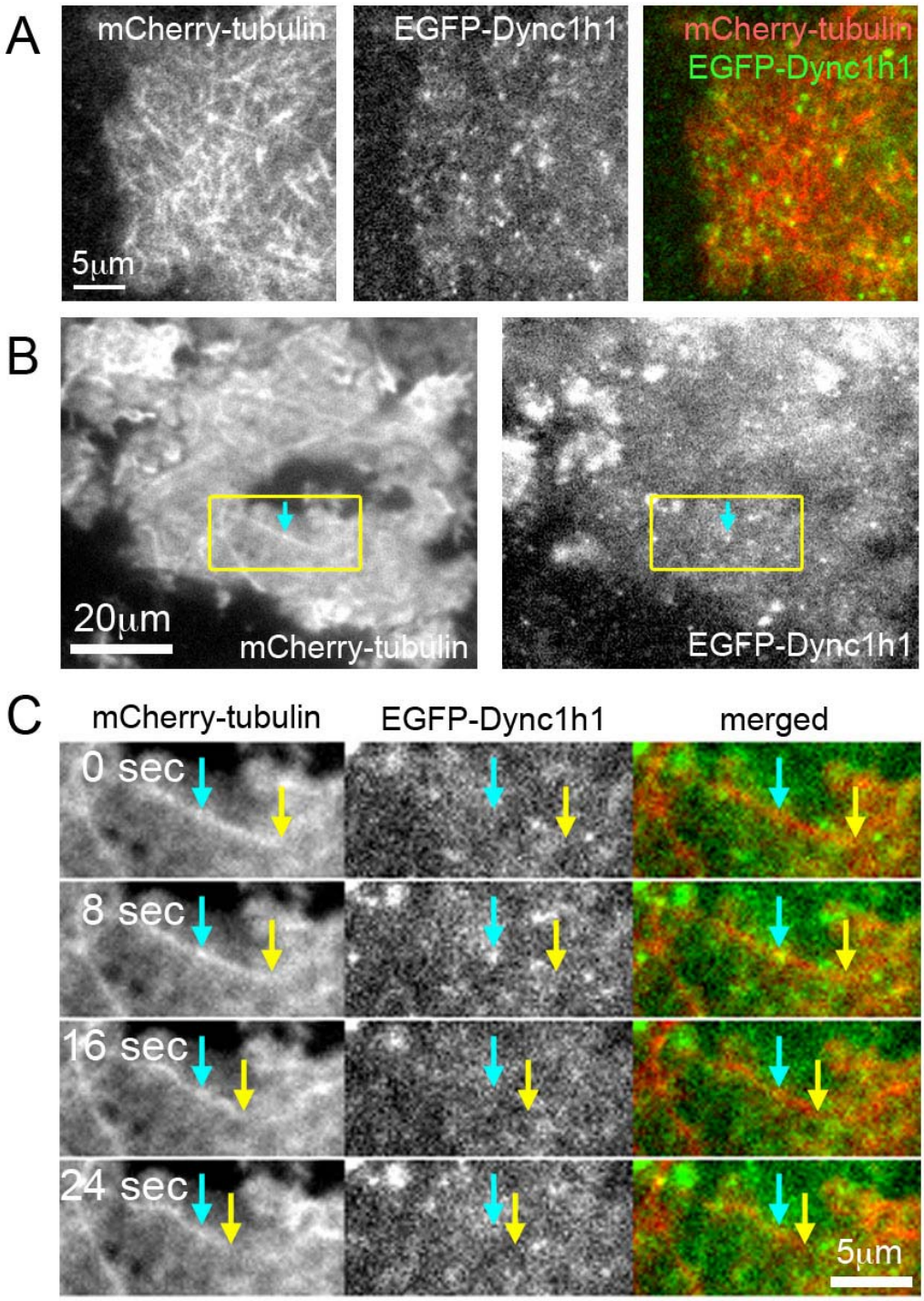

Figure S6: Observation of dynamic behavior of microtubules labeled directly using mCherry-tubulin in COS7 cells without nocodazole washout via TIRF microscopy. A) In the majority of cells, microtubule density was very high in the TIRF field and dynamic microtubule behaviors were difficult to evaluate (see also Movie 4). B) Example of a cell, in which an apparent movement of an individual microtubule colocalizing with a dynein speckle (cyan arrow) was detectable. C) Enlarged view of the boxed region shown in B. The presence of the colocalized dynein speckle correlates with microtubule movements.

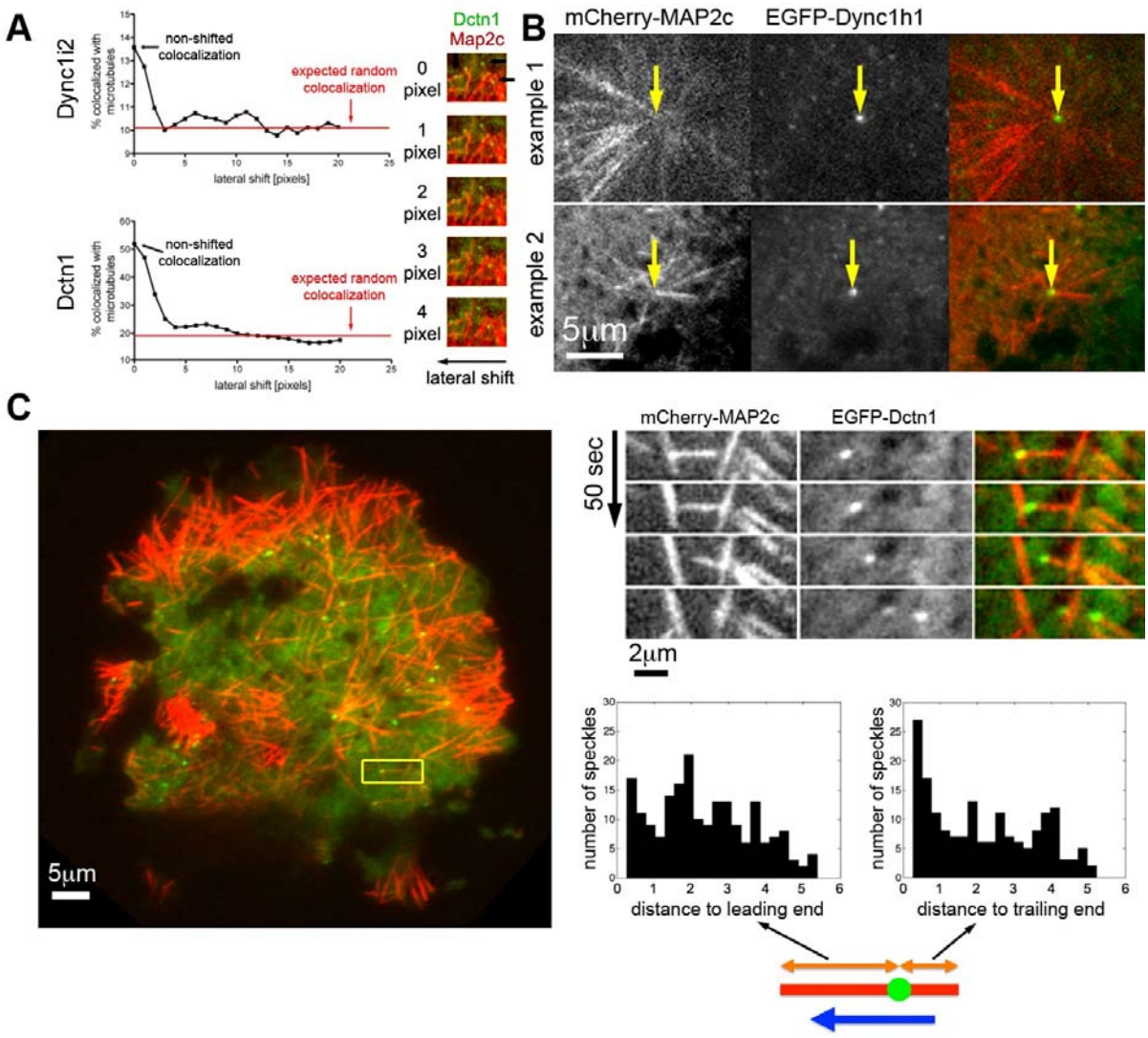

Figure S7: Colocalization of dynein subunits with microtubules. A) Left: Colocalization of the dynein intermediate chain (Dync1i2) and the dynactin subunit Dctn1 (p150glued) with short microtubules during nocodazole washout. Analysis was performed analogous to Figure 3B. The colocalization of Dctn1 with microtubules is higher, presumably due to its ability to directly bind microtubules. Right: A small region from a lateral shift series. Overlap between dynactin speckles and short microtubules was lost after the respective images were shifted by a few pixels against each other. B) Accumulation of the dynein heavy chain at the center of microtubule asters. After nocodazole washout in mCherry-MAP2c transfected COS7 cells, the centers of microtubule asters were usually not within the evanescent wave of the TIRF microscope. However, in the two examples shown here, asters approached the TIRF field and an accumulation of the EGFP-labeled dynein heavy chain Dync1h1 was detected at their center. C) Accumulation of dynactin at the

trailing end of short microtubules. Left: A mCherry-MAP2c/EGFP-Dctn1 co-transfected COS7 cell shortly after nocodazole washout. Right top: Enlargement of yellow box from the left panel. A motile dynactin speckle is continuously located at the trailing end of a motile short microtubule. Right bottom: Histograms of the measured distance from the speckle to the leading or trailing end of the short microtubule. Speckles were predominantly near the trailing end (peak in right histogram at distance=0).

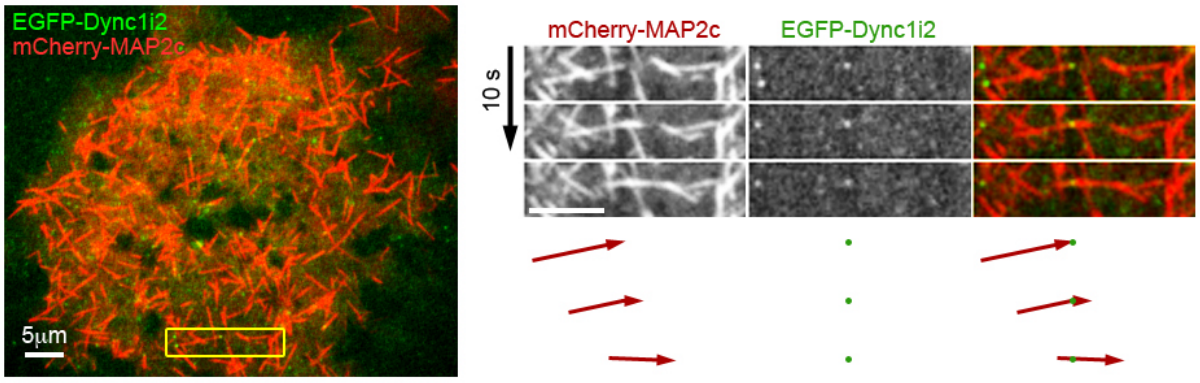

Figure S8: A microtubule pivots around a speckle of the dynein intermediate chain (Dync1i2). Left: A mCherry-MAP2c/EGFP-Dync1i2 co-transfected COS7 cell shortly after nocodazole washout. Right: Enlargement of yellow box from the left panel. A motile microtubule slightly changes its angle while it slides along a speckle of the dynein intermediate chain. The movement of microtubule on stationary dynein speckle is indicated with red arrows and green dots, respectively (see also Movie 8 in supplementary material).

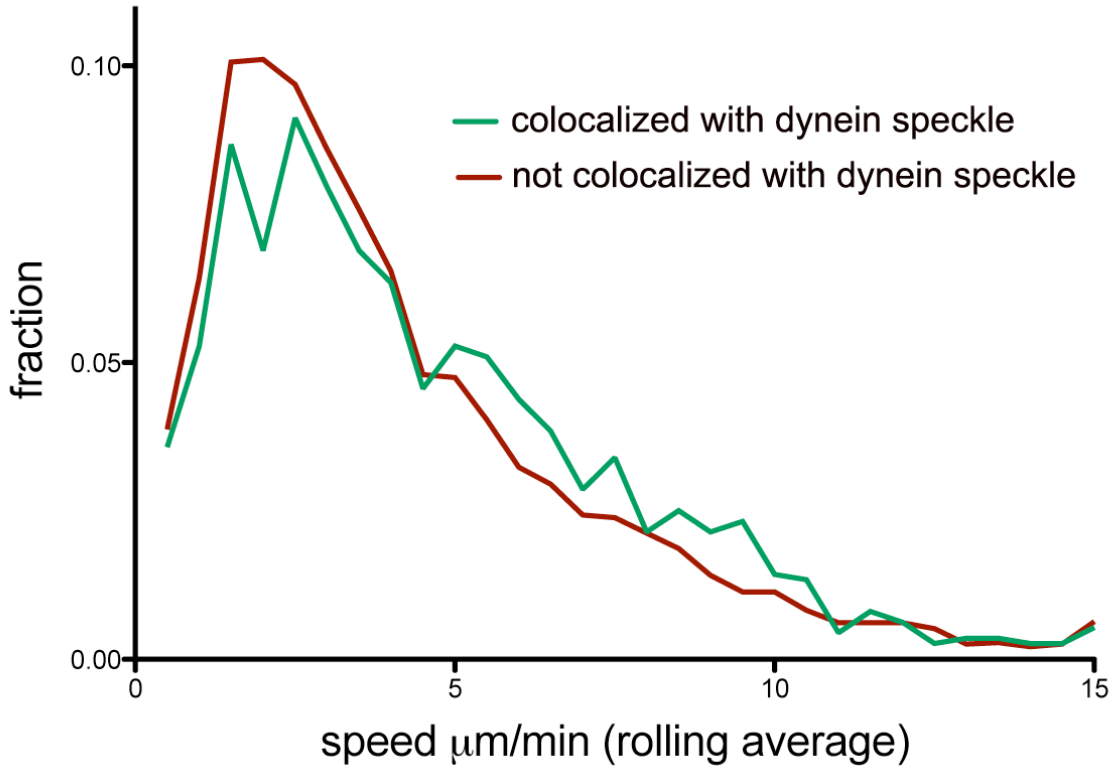

Figure S9: Histogram of microtubule speed distributions. Microtubules were either colocalized with dynein speckles (green) or not (red). Most of the observed microtubule movements are small displacements corresponding to Brownian motion. Larger displacements are more common in microtubules associated with dynein speckles. To suppress the effect of random Brownian motion, microtubule speeds are calculated as a rolling average of 4 frames.

Supplementary Movie Legends:

Movie 1: Directional sliding of microtubules near the cell cortex observed via wide-field (left) and TIRF (right) imaging.

Movie 2: Polarity orientation of motile microtubules observed via wide-field and TIRF imaging. This example shows multiple motile microtubules, which were labeled at their plus-tips with mCherry-EB3 and with EGFP-MAP2c along their entire length. Top left: combined mCherry-EB3 TIRF (green) and EGFP-MAP2c TIRF (red); Top right: mCherry-EB3 TIRF; Bottom left: EGFP-MAP2c TIRF; Bottom right: EGFP-MAP2c wide-field.

Movie 3: Directional sliding of microtubules in COS7 cells transfected with various microtubule associated proteins. COS7 cells were transfected with EGFP-MAP2c, EGFP-tau, or EGFP-EMAP115-MTBD. Microtubule motility was observed either via wide-field or TIRF imaging shortly after nocodazole washout.

Movie 4: Microtubules labeled directly with mCherry-tubulin in COS7 cells. As microtubules were very dense, dynamic, long and flexible, potential movements were difficult to interpret. Cells were co-transfected with EGFP-Dync1h1 to simultaneously visualize cortical dynein complex dynamics.

Movie 5: Dynamic colocalization of microtubules and dynein heavy chain speckles. This example shows a motile dynein speckle colocalized with a microtubule that is first stationary (case 2) and later becomes mobile.

Movie 6: Dynamic colocalization of microtubules and dynein heavy chain speckles. This example shows stationary dynein speckles colocalized with motile microtubules (case 3).

Movie 7: Dynamic colocalization of microtubules and dynein heavy chain speckles. This is another example of a stationary dynein speckle colocalized with a motile microtubule (case 3).

Movie 8: Dynamic colocalization of microtubules and dynein heavy chain speckles. This example shows a motile dynein speckle located at the trailing microtubule end, which moves together with the motile microtubule (case 5).

Movie 9: Correlation of microtubule and dynein speckle dynamics. A microtubule slightly rotates while it slides over a speckle of the dynein intermediate chain in the middle of this region. The pivot point of the microtubule rotation is located at the dynein intermediate chain speckle (see also Figure S8 in supplementary material).

Movie 10: Correlation of microtubule and dynein speckle dynamics. The disappearance of a dynein heavy chain speckle at timepoint 51 s coincides with the loss of a kink in a microtubule.

Movie 11: Stochastic simulation of dynein mediated microtubule motility in cells. Left: Stochastic simulation of microtubule (yellow) movements powered by cortical dynein speckles (blue). Right: Movie of microtubule movements following nocodazole washout.